Desalination and Water Treatment
www.deswater.com
doi: 10.5004/dwt.2023.30179

316 (2023) 111–120
December

Study on visible photocatalytic activity of an oxalate-extended Co(II) coordination polymer

Jia-Jia Zhang[a,†], Jian-Hui Liu[b,†], Yu-Chang Wang[c], Wen-Fu Yan[d], Yuan-Peng Wang[a], Yu Han[a], Jia-Tong Qu[a], Juan Jin[a,d,*], Yong-Feng Liu[a], Jun-Shen Liu[a,*]

[a]*School of Chemistry and Materials Science, Ludong University, Yantai, Shandong 264025, China, emails: 2639358348@qq.com (J.-J. Zhang), 1925844133@qq.com (Y.-P. Wang), 3293227809@qq.com (Y. Han), 3558836805@qq.com (J.-T. Qu), jinjuan8341@163.com (J. Jin), 37154690@qq.com (Y.-F. Liu), liujunshen@163.com (J.-S. Liu)*
[b]*Yantai Center of Ecology and Environment Monitoring of Shandong Province, email: lyliujianhui@163.com (J.-H. Liu)*
[c]*Yantai Valiant Fine Chemicals Co., Ltd., Yantai, Shandong 264006, China, email: yuchang8341@163.com (Y.-C. Wang)*
[d]*College of Chemistry and State Key Laboratory of Inorganic Synthesis and Preparative Chemistry, Jilin University, Changchun, Jilin 130023, China, emails: jinjuan8341@163.com (J. Jin), yanw@jlu.edu.cn (W.-F. Yan)*

Received 27 July 2023; Accepted 28 November 2023

ABSTRACT

A two-dimensional (2D) coordination polymer [Co(ox)(bpy)] **1** (ox = oxalate, bpy = 4,4′-bipyridine) was prepared by hydrothermal synthesis using $CoCl_2{\cdot}5H_2O$, oxalic acid, bpy as raw material. Compound **1** is a 2D structure extended by ox and bpy, and it has excellent visible photocatalytic performance. The photocatalytic efficiency of compound **1** could reach up to 98.13% with pH = 10 when two drops of H_2O_2 were added to methylene blue. The photocatalytic degradation results could be described by the first-order kinetic. Besides, after five cycles, the degradation efficiency decreased only 4.11% (without H_2O_2) and 5.22% (with H_2O_2). Meanwhile, the solid fluorescence and UV-Visible diffuse reflection of compound **1** were also studied. What's more, the visible light photocatalytic mechanism of compound **1** was analyzed more clearly by free radical trapping experiment and Mott–Schottky curve.

Keywords: Water pollution; Coordination polymer; Oxalate; Photocatalysis; Visible light

1. Introduction

In recent years, printing and dyeing water pollution has become more and more serious with the rapid development of industry, which not only destroys the ecological environment, but also has a serious impact on human health. In order to solve this problem, people have taken many methods to purify sewage, for example membrane separation [1], adsorption method [2], activated sludge treatment, biological treatment [3], etc. Although these methods have yielded some results, they all have a number of drawbacks as well. For instance, the membranes of membrane separation technology are easy to form an attachment layer, which affects the purification results [4]. And the main disadvantage of adsorption method is easy to reach adsorption saturation, and exists secondary pollution [5]. The operation of activated sludge process is complicated and it is easy to produce a large amount of sludge [6]. Biological treatment is costly and inefficient [7]. The emergence of photocatalysis has effectively solved the above problems. In the past several years, photocatalysis have made many achievements in dyeing wastewater treatment. George et al. [8] prepared Co-doped ZnO nanomaterials to perform photocatalytic degradation of dyes and found that the degradation rate was 70% after 60 min. Aravinthkumar et al. [9] synthesized Cr:STO-7 material and used it for visible light photocatalytic

* Corresponding authors.
† Both the authors contributed equally to this work.

degradation of methylene blue (MB). The degradation efficiency was up to 88% at 120 min. Therefore, the key of photocatalysis is the choice of photocatalyst. Titanium dioxide and zinc oxide are commonly used photocatalysts, but these photocatalysts have shortcomings such as low quantum conversion efficiency and narrow response spectrum range [10]. Consequently, researching and developing new photocatalysts has become a focal point of domestic and international research.

It is found that the structure of coordination polymer is diverse and its physical and chemical properties are superior, so it is widely used in catalysis, medicine, magnetism and so on [11]. Especially in photocatalysis, coordination polymers take full their advantages of high specific surface area, high coordination pattern and orderly structure [12]. Hu et al. [13] synthesized two novel coordination polymers ([Zn(L)(2,2′-bipy)], [Zn(L)$(bbi)_{0.5}$]) for photocatalytic degradation of organic dyes. For the first compound, the efficiency of degradation of the dye template was found to be 65.44% after 100 min. The degradation efficiency was 78.54% for the second compound. Lu et al. [14] synthesized coordination polymers with three different ligands {[Ni$(L^1)_{1.5}$(HBTC)(H_2O)], [Ni$(L^2)_2$(HBTC)]×2H_2O, [$Cu_2(L^2)_{0.5}$(BTC)(μ_3-OH)]×2H_2O} and their degradation rates of CR (Congo red) were 93.10%, 44.25%, 90.85%, respectively [14]. However, there are few reports on photocatalytic degradation of organic dyes under visible light. In order to obtain visible light responsive photocatalytic coordination polymers, it is a very good idea to select inorganic metal ions with good catalytic activity as well as conjugated organic ligands with good photophysical properties. Oxalic acid (H_2ox) is a conjugated system with large π bonds. This structural advantage plays an important role in the synthesis of coordination polymers and enhances the photocatalytic degradation efficiency under visible light. Dridi et al. [15] synthesized a Cd(II) coordination polymer with ox (ox = oxalate) ligand and investigated its photocatalytic performance. 4,4′-bipyridine (bpy) plays an important role in the construction of coordination polymers due to the symmetric N atoms on the two benzene rings in its structure. More importantly, its structural advantage of having a large π-bonded conjugated system also facilitates the photocatalytic performance under the visible light. Hou et al. [16] chose bpy to synthesize the polymer and found that the polymer had superior photocatalytic degradation properties for methyl orange and methylene blue. Co^{2+} also have strong catalytic activity. Muslim et al. [17] synthesized coordination polymer of Co^{2+} for degradation of organic dyes. Therefore, we selected Co^{2+} as the central metal, H_2ox and 4,4′-bpy as ligands to synthesize a coordination polymer [Co(ox)(bpy)] **1** and investigated its photocatalytic degradation effect. It was found that compound **1** had superior photocatalytic performance under the visible light. Finally, when added H_2O_2 in methylene blue (MB), the visible photocatalytic performance of compound **1** could reach 98.13% with pH = 10 at 70 min. This degradation effect is higher than that of some photocatalysts previously reported [18,19]. After 5 cycles, the photocatalytic efficiency of compound **1** decreased by 5.22% and 4.11%, respectively with and without H_2O_2, and X-ray diffraction (XRD) showed that the structure of compound **1** was stable. In conclusion, compound **1** is a potential visible light photocatalyst.

2. Experimental section

2.1. Materials and characterization

Raw materials used in this experiment were purchased commercially without further processing. The elemental analysis was carried out on a PerkinElmer 2400 LS II Elemental Analyzer (PerkinElmer Enterprise Management (Shanghai) Co., Ltd., 1670 Zhangheng Road, Zhangjiang Hi-Tech Park, Shanghai, China). A Perkin Elmer Spectrum One FTIR Spectrometer was used to record the infrared spectra in the 4,000–400 cm^{-1} range of the powder samples on a KBr plate. The thermogravimetric (TG) property was determined on a PerkinElmer TGA 7 Instrument (PerkinElmer Instruments (Shanghai) Co., Ltd., Building 4, Lane 67, Libing Road, Zhangjiang Hi-Tech Park, Shanghai, China) that was heated in air at a rate of 10°C/min. An LS 55 fluorescence/phosphorescence spectrophotometer was used to measure the solid-state fluorescence spectra at room temperature. UV-Vis diffuse reflectance spectra (DRS) was recorded using a SolidSpec-3700 UV-Vis spectrophotometer in the 240–800 nm range with $BaSO_4$ baseline correction. The absorbance of the MB solution was measured using a 722E type visible spectrophotometer with an absorption wavelength of 664 nm, and the photocatalytic degradation efficiency (DE) of compound **1** was calculated according to Eq. (1).

$$\frac{\left(A_t - A_0\right)}{A_0} = \mathrm{DE} \tag{1}$$

2.2. Synthesis of compound **1**

2.2.1. [Co(ox)(bpy)] **1**

A mixture of $CoCl_2{\cdot}5H_2O$ (0.50 mmol, 118 mg), 4,4′-bpy (0.50 mmol, 78 mg), H_2ox (0.50 mmol, 63 mg) were dissolved into H_2O (15 mL). The mixture was stirred for 4 h at ambient temperature Its pH was then adjusted to 5 with saturated oxalic acid solution. The obtained mixture was sealed in a 25 mL Teflon autoclave reactor and heated at 170°C for 4 d under autogenous pressure. The red crystals were finally got in 45% yield (based on Co(II)). Anal. Calcd. for $C_{12}H_8N_2O_4Co$ (%): C, 44.85; H, 2.25; N, 5.78. Found: C, 43.24; H, 2.68; N, 6.18. IR (cm^{-1}): 3,440 s, 2,358 s, 1,600 s, 1,530 s, 1,409 w, 1,326 s, 1,220 s, 768 m, 684 w, and 517 m.

2.3. X-ray crystallography

A Siemens SMART CCD diffractometer (Siemens (China) Co., Ltd., 7 Wangjing Zhonghuan South Road, Chaoyang District, Beijing, China) with Mo-Kα radiation (λ = 0.71073 Å) was used to collect crystallographic data for compound **1**. The structure has been solved by direct methods using the program SHELXTL and it has been specified on F^2 using the package SHELXL-2014 by means of full-matrix least-squares methods. The non-hydrogen atoms of compound **1** are anisotropic and the hydrogen atoms of the ligand are in the calculated positions. CCDC number is 2285086. The crystallographic data of compound **1** is shown in Table 1.

2.4. Photocatalytic degradation

MB was used to test the photocatalytic degradation rate of the compound **1** under visible light. Prepare MB solution

Table 1
Crystallographic data for compound 1

Compound	1
Formula	$C_{12}H_8N_2O_4Co$
M	303.13
Crystal system	Orthorhombic
Space group	I_{mmm}
a (Å)	5.4021(5)
b (Å)	10.9756(11)
c (Å)	11.3896(10)
a (°)	90
b (°)	90
g (°)	90
V (Å^3)	675.30(11)
Z	2
D_c (g/cm^3)	1.491
m (Mo-Ka) (mm^{-1})	1.280
F (000)	306
Total data	1,531
Unique data	366
R_{int}	0.0205
GOF	1.452
R_1 ($I > 2\sigma(I)$)	0.0355
wR_2 (all data)	0.1241

with the absorbance of **1** and adjust its pH to 4, 7, 10 with NaOH and H_2SO_4. 40 mg of compound **1** was dissolved in 80 mL MB solution and treated in the dark for 30 min to achieve the equilibrium of adsorption and desorption. Finally, the solution was irradiated with a xenon lamp and visible light for 70 min. The samples were removed every 10 min and centrifuged to measure the absorbance.

3. Results and discussion

3.1. Hydrothermal synthesis of coordination polymer

Hydrothermal synthesis is one of the most commonly method for compound synthesis. In the process of hydrothermal synthesis, the factors affecting crystal growth are reaction time, temperature and pH. So, we explored the optimal reaction conditions for compound synthesis. Compound **1** was heated at 170°C for 4 d. The crystals shape are regular and have high purity at pH = 5.

3.2. Structural description

The crystal structure analysis reveals that compound **1** is a two-dimensional (2D) layer Co^{2+} coordination polymer with H_2ox and bpy ligands. Its space group is I_{mmm}. As shown in Fig. S1, the asymmetric unit of compound **1** includes one Co^{2+}, two H_2ox molecules and two bpy molecules. Co^{2+} is located in a six-fold coordination field as a center metal consisting of two N atoms on bpy (N1, N1b) and four O atoms on H_2ox (O1, O1b, O1d, O1i). The bond of Co-O_{Ox} is 2.085 (3) and Co-N_{bpy} is 2.154 (5). These are comparable to the reported bond lengths of the compounds [20,21]. As shown in Fig. 1, the N atoms on bpy bind the central metal Co^{2+} to form a one-dimensional (1D) chain structure in the *c*-direction. H_2ox adopt μ_2 coordination mode and extend the 1D chain into a 2D layer structure in the *ac* direction by four oxygen atoms (O1d, O1i, O1j, O1k) (Fig. 2).

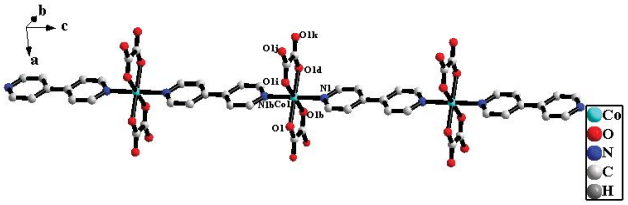

Fig. 1. One-dimensional chain structure for compound 1 (symmetric code b: *x*, –*y* + 1, –*z*; d: –*x* + 1, –*y* + 1, *z*; i: –*x* + 1, *y*, –*z*; j: *x*–1, *y*, *z*, *k*: *x*–1, –*y* + 1, –*z*; l: *x*, *y*, *z*–1).

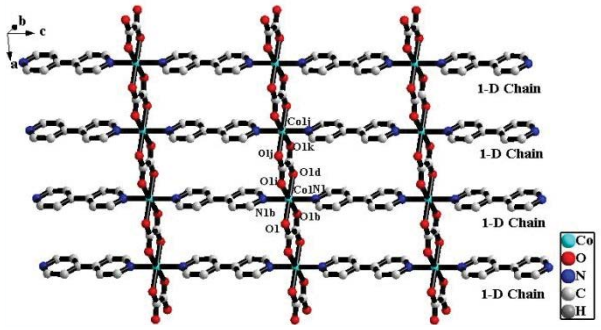

Fig. 2. Two-dimensional layer structure for compound 1 (symmetric code b: *x*, –*y* + 1, –*z*; d: –*x* + 1, –*y* + 1, *z*; i: –*x* + 1, *y*, –*z*; j: *x*–1, *y*, *z*, *k*: *x*–1, –*y* + 1, –*z*; l: *x*, *y*, *z*–1).

3.3. IR analysis

As shown in Fig. S2, the infrared absorption peak of compound **1** is 3,440 s, 2,358 s, 1,600 s, 1,530 s, 1,409 w, 1,326 s, 1,220 s, 768 m, 684 w, and 517 m. Compound **1** has an infrared absorption peak at 1,600 cm^{-1}, which is the stretching vibration peak of carboxyl group, indicating that during the formation of compound **1**, carboxyl acid has a coordination with metal [22]. There are distinct peaks at 1,530 and 1,220 cm^{-1} attributed to C=N and C–N stretching vibrations, respectively, which indicate 4,4′-bpy was successfully coordinated with the metal during the synthesis of compound **1** [23].

3.4. TG analysis

The thermogravimetric analysis of compound **1** was tested at 60°C–800°C (Fig. 3). It was found that compound **1** underwent one-step weight loss in the range of 320°C–400°C. The weight loss in this step was attributed to the loss of all ligands (Found: 73.10%, Calcd: 75.29%). The final remaining product is CoO (Found: 26.90%, Calcd: 24.71%).

3.5. Solid fluorescence analysis

As shown in Fig. 4, the emission peak of **1** is 423 nm, with a certain redshift compared to H_2ox (λ_{em} = 335 and

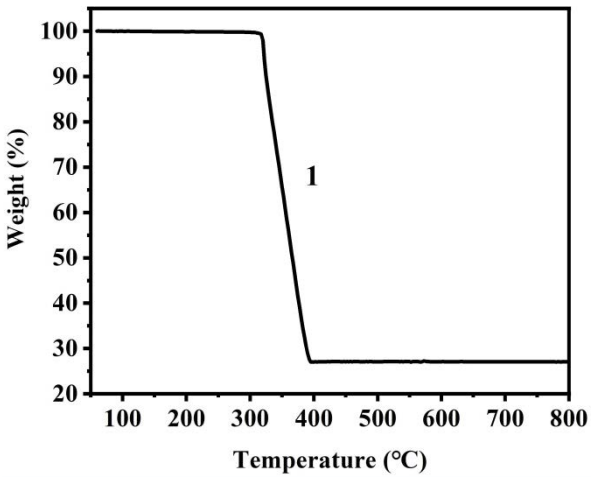

Fig. 3. Thermogravimetric curve of compound 1.

350 nm) and bpy (λ_{em} = 359 nm), which may be related to the charge transfer from the ligand to the metal (LMCT) [24–26].

3.6. UV-Vis absorption spectra and band gap

The UV-Visible diffuse reflection of compound **1** was tested between 240–800 nm at room temperature. It can be seen from Fig. 5 that compound **1** has a certain absorption intensity between 400–800 nm, indicating that compound **1** has a light response at visible light Eq. (2):

$$\left(\alpha h\upsilon\right)^{1/n} = A\left(h\upsilon - E_g\right) \tag{2}$$

where α is absorption index, h is Planck constant, υ is frequency, A is constant [27]. The band gap energy E_g = 2.6 eV is calculated. Since compound **1** with a narrow gap band can produce electron–hole pairs from low-energy photons, it can exhibit better photocatalytic properties.

3.7. Photocatalytic property

3.7.1. Effect of solution pH and addition of H_2O_2 on photocatalysis

MB was selected as the template of organic dye and the photocatalytic activity of the compound **1** was tested by calculating MB's absorbance. Researches had shown that there are a number of factors could affect photocatalysis. pH is a critical condition, so we studied the photocatalytic effect of compound **1** at three different pH (pH = 4, 7, and 10). As shown in Fig. 6, with the increase of pH, the photocatalytic degradation efficiency of compound **1** increases continuously (pH = 4: 50.90%; pH = 7: 67.87%; pH = 10: 75.40%). The self-degradation rate of MB was pH = 4: 11%; pH = 7: 28.2%; pH = 10: 31.5% (Fig. S3). This is likely because electrons are generated on the surface of the catalyst when exposed to visible light. With the increases of pH, there will be more OH^- in the solution. OH^- will be reduced to hydroxyl radicals by electrons, which can hinder the recombination of electrons and holes. Thus, the photocatalytic performance is improved [28]. H_2O_2 is also

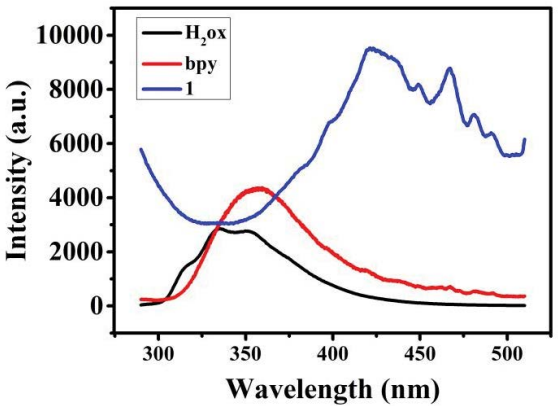

Fig. 4. Solid-state photoluminescence emission spectra of compound 1, H_2ox and bpy.

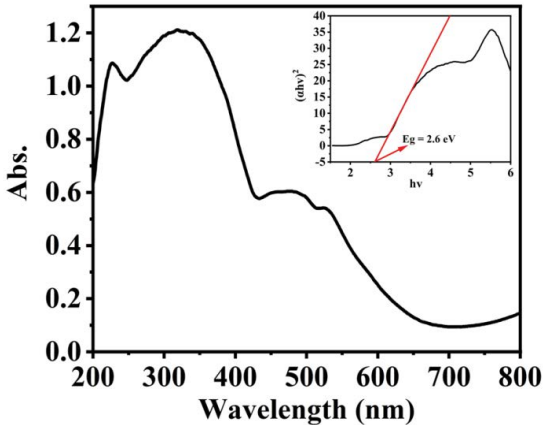

Fig. 5. UV-Vis absorption spectra and Tauc plots of compound 1.

an important factor affecting the photocatalytic performance, so the photocatalytic degradation efficiency with and without H_2O_2 was compared. As shown in Fig. 6, it is found that the degradation efficiency of adding H_2O_2 (pH = 4: 70.19%; pH = 7: 91.10%; pH = 10: 98.13%) is higher than that without adding H_2O_2 (pH = 4: 50.90%; pH = 7: 67.87%; pH = 10: 75.40%) at the same pH. This is because H_2O_2 can generate $^{\bullet}OH$ under the visible light, which can increase the efficiency of photocatalytic degradation [29].

3.7.2. Kinetic model of photocatalytic reaction

The experimental results showed that the photocatalytic degradation efficiency became better and better with the increase of time within 70 min. Therefore, a first-order kinetic study was conducted on the degradation results, and it was found that the photocatalytic degradation effect and time could be described by Eq. (3):

$$\ln\left(\frac{C_0}{C_t}\right) = kt \tag{3}$$

where C_0 is the initial absorbance of MB, C_t is the absorbance of compound **1** to MB at time t, and k is the rate constant

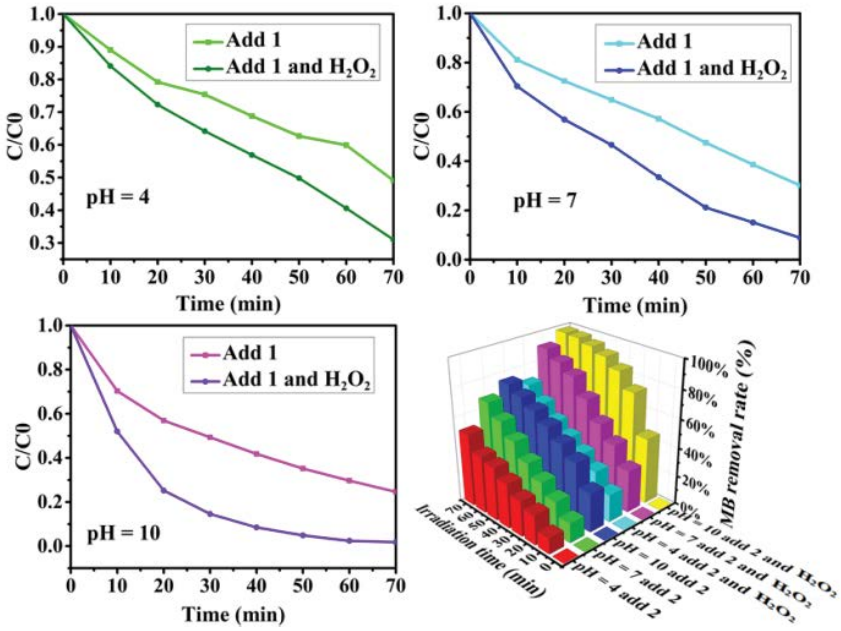

Fig. 6. Methylene blue degradation profile of different conditions under visible light irradiation.

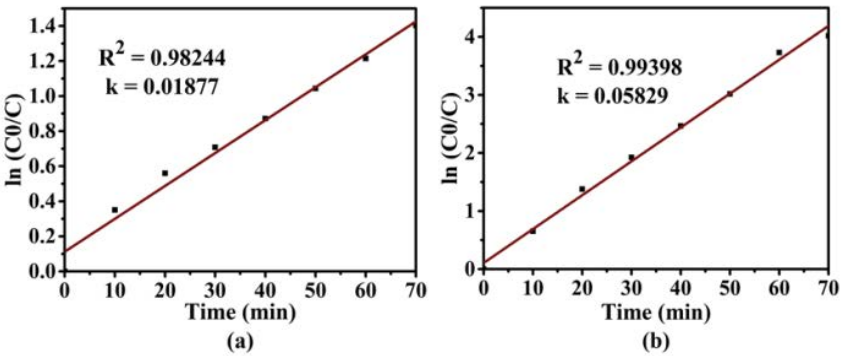

Fig. 7. Determination of kinetic parameters. Conditions: pH = 10, add compound 1 for (a) and pH = 10, add compound 1 and H_2O_2 for (b).

[30]. As shown in Fig. 7, under different conditions with and without H_2O_2, the *k* is 0.01877 and 0.05829, respectively.

3.7.3. Recyclability of catalyst

In order to study the stability of the compound **1**, five cyclic degradation experiments were carried out. The results showed that the degradation efficiency decreased by 4.11% when H_2O_2 was not added and by 5.22% when H_2O_2 was added (Fig. 8). After these five cycles degradation experiments, degradation efficiency decreased to a certain extent, which may be because there was a certain loss of samples in each recycling experiment.

3.7.4. XRD analyses

The purity of the synthesized sample and the crystal state after five times of recycling were analyzed by XRD (Fig. 9). The XRD spectra obtained by single crystal data simulation are consistent with those obtained experimentally, indicating that the synthesized compound **1** is a pure phase. The spectra of the samples obtained after 5 cycles of recovery was also relatively consistent, which declared that the framework of compound **1** was well maintained.

3.8. Analysis of photocatalytic mechanism

3.8.1. Free radical capture experiments

In order to investigate which active substance plays a role in the whole tube catalysis process, we conducted a free radical capture experiment. p-benzoquinone (PBQ) was used as superoxide radical trapping agent, isopropyl alcohol (IPA) as hydroxyl radical trapping agent, EDTA as hole trapping agent [31]. As shown in Fig. 10, the comparison of experimental results shows that the degradation efficiency decreases by 0.1% when PBQ is added and by 6.8% when IPA is added. The degradation rate of MB was reduced less

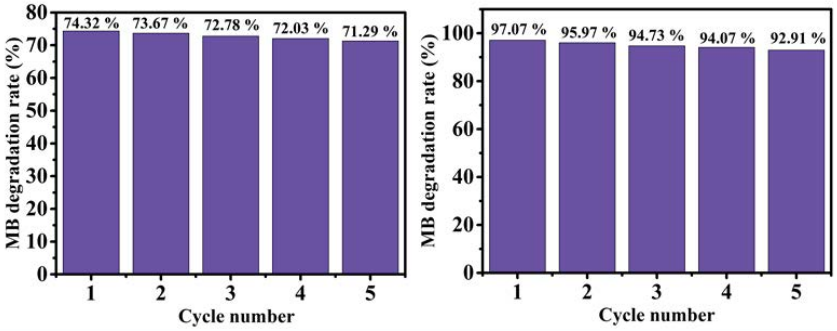

Fig. 8. Recycling experiments in methylene blue photodegradation for compound 1. Conditions: pH = 10, add compound 1 for (a) and pH = 10, add compound 1 and H_2O_2 for (b).

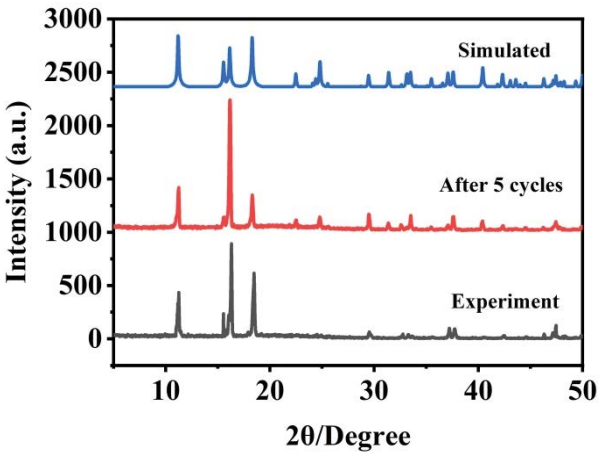

Fig. 9. X-ray diffraction patterns of compound 1.

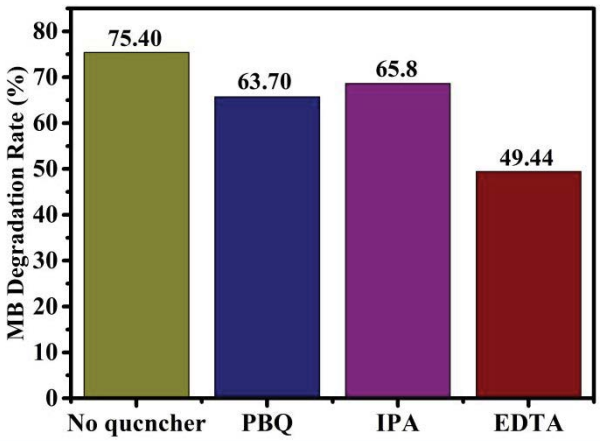

Fig. 10. Photocatalytic degradation efficiency of methylene blue by compound 1 in different scavengers.

when the two trapping agents were used. However, when EDTA was added, the reduction efficiency decreased by 25.96%, which was a large decrease. Therefore, holes played a leading role in the photocatalytic process.

3.8.2. Mott–Schottky curve

The Mott–Schottky curve of compound **1** was tested in order to understand the band energy level of compound **1** and to provide a clearer explanation of the photocatalytic mechanism of compound **1**. Fit Mott–Schottky's curve, if the slope is negative, compound **1** is a *p*-type semiconductor, and if the slope is positive, it is an *n*-type semiconductor. Fig. 11 shows that compound **1** is an *n*-type semiconductor and has a flat-band potential of –0.49 eV. For n-type semiconductors, the conduction band (CB) potential is 0.1 eV smaller than the flat band potential [32]. So, the CB potential is –0.59 eV vs. Ag/AgCl. Its CB potential with respect to the hydrogen electrode (–0.393 V) is calculated from the equation $E_{NHE} = E_{Ag/AgCl} + 0.197$ V [33]. This is lower than the potential which O_2 is reduced to $^{\bullet}O_2^-$ (–0.33 eV). So, step (II) can occur. Compound **1** has $E_g = 2.6$ eV, so its valence band (VB) is 2.207 eV (vs. NHE). This value is greater than the value for the oxidation of OH^- to $^{\bullet}OH$ (1.99 eV) and less than the value for the reduction of H_2O to $^{\bullet}OH$ (2.38 eV) [34], so step

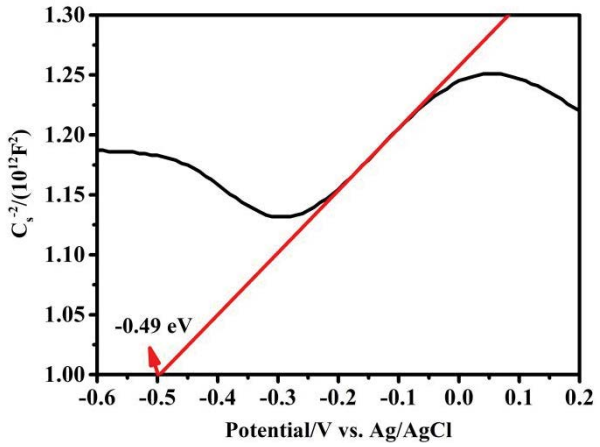

Fig. 11. Mott–Schottky plots of compound 1.

(II) can proceed. In summary, the visible light photocatalytic mechanism of compound **1** was deduced as follows (Fig. 12).

$$CP - Co + hv \rightarrow h^+ + e^- \quad (I)$$

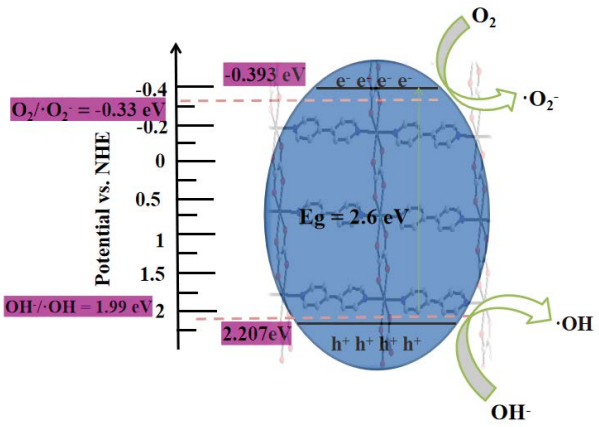

Fig. 12. Possible photocatalytic mechanism of compound 1 in visible light.

$$O_2 + e^- \rightarrow {}^{\bullet}O_2^- \quad \text{(II)}$$

$$OH^- + h^+ \rightarrow {}^{\bullet}OH \quad \text{(III)}$$

$${}^{\bullet}O^{2-} + MB \rightarrow \text{oxidation productions} \quad \text{(IV)}$$

$${}^{\bullet}OH + MB \rightarrow \text{oxidation productions} \quad \text{(V)}$$

$$h^+ + MB \rightarrow \text{oxidation productions} \quad \text{(VI)}$$

$$H_2O_2 + e^- \rightarrow OH^- + {}^{\bullet}OH \quad \text{(VII)}$$

4. Conclusions

In short, [Co(ox)(bpy)] **1** was prepared via facile hydrothermal synthesis. Through the analysis of its structure and properties, we can come to some conclusions as follows: (i) H_2ox and bpy ligands extend compound **1** into a 2D structure. (ii) TG analysis showed that compound **1** lost weight in one step at 320–400°C and had good thermal stability. (iii) The solid fluorescence of compound **1** has a certain red shift compared to the ligand, which is caused by the charge transfer from the ligand to the metal. (iv) The UV-visible diffuse reflectance of compound **1** was analyzed and its E_g = 2.6 eV, which indicates that **1** had a light response in the visible region. (v) Importantly, compound **1** has superior photocatalytic property under the visible light. MB degradation efficiency could reach 98.13% and degradation results were consistent with the first-order kinetic model. (vi) Compound **1** was used for cycle degradation of MB. After 5 cycles, it was found that the degradation effect decreased by 4.10% (without H_2O_2) and by 5.22% (with H_2O_2), which indicated its repeatability was fine. More importantly, XRD showed that the structure of compound **1** did not change after five cycles. (vii) Through free radical capture experiments, we found that hydroxyl radicals, superoxide radicals and holes all played roles in the whole photocatalytic degradation process, but holes were dominant in the whole process. (viii) The visible light photocatalytic mechanism of compound **1** was analyzed more clearly by Mott–Schottky curve. Therefore, the photocatalytic experiments showed that compound **1** is a potential photocatalyst for visible light.

Acknowledgement

This research was supported by the Natural Science Foundation of Shandong Province (No. ZR2017PB006), the Open Foundation of State Key Laboratory of Inorganic Synthesis and Preparative Chemistry of Jilin University (No. 2023-20), the Natural Science Foundation of Ludong University (No. LY2014015), the Innovation Foundation for Students of Ludong University (No. ld17l040), the National Natural Science Foundation of China (No. 21961027), the Teaching Reform Research Project of Undergraduate Universities in Shandong Province (No. M2022181), the Teaching Reform Research Project of Shandong Chemical Teaching Committee (No. SDHX-YB-2022-25).

References

[1] L. Yuan, Application research of non-immersed ultrafiltration membrane separation devices in rural decentralized water supply projects, Int. Core J. Eng., 8 (2022) 618–621.
[2] X. Hu, F. Alsaikhan, H.Sh. Majdi, D.O. Bokov, A. Mohamed, A. Sadeghi, Predictive modeling and computational machine learning simulation of adsorption separation using advanced nanocomposite materials, Arabian J. Chem., 15 (2022) 104062, doi: 10.1016/j.arabjc.2022.104062.
[3] Y.-P.Wang,Y.-C.Guo,J.Lu,Y.-C.Wang,W.-F.Yan,J.Jin,W.-T.Zhang, J.-J. Zhang, Q.-F. Yang, Q.-A. Qiao, Synthesis, structure and photocatalytic property of a novel Zn(II) coordination polymer based on *in situ* synthetized 4,4′-hexafluoroisoprorylidene-diphthalhydrazidate ligand, J. Mol. Struct., 1294 (2023) 136338, doi: 10.1016/j.molstruc.2023.136338.
[4] J.J. Xing, H. Liang, S.Q. Xu, C.J. Chuah, X.S. Luo, T.Y. Wang, J.L. Wang, G.B. Li, S.A. Snyder, organic matter removal and membrane fouling mitigation during algae-rich surface water treatment by powdered activated carbon adsorption pretreatment: enhanced by UV and UV/chlorine oxidation, Water Res., 159 (2019) 283–293.
[5] Y.C. Guo, Z.Y. Jiang, Y.C. Wang, J. Jin, W.F. Yan, Z.X. Zhao, Y.M. Ma, L.Y. Yan, Z.Q. Jiang, Q.A. Qiao, Synthesis, structure and photocatalytic property of the 1D oxalate-bridged coordination polymer of manganese(II), J. Mol. Struct., 1251 (2022) 131961, doi: 10.1016/j.molstruc.2021.131961.
[6] W.H. Chen, J.H. Xiong, X. Teng, J.X. Mi, Z.B. Hu, H.F. Wang, Z.F. Chen, A novel heterogeneous Co(II)-Fenton-like catalyst for efficient photodegradation by visible light over extended pH, Sci. China Chem., 63 (2020) 1825–1836.
[7] K.T. Kubra, Md.S. Salman, Md.N. Hasan, Enhanced toxic dye removal from wastewater using biodegradable polymeric natural adsorbent, J. Mol. Struct., 328 (2021) 115468, doi: 10.1016/j.molliq.2021.115468.
[8] N.S. George, L.M. Jose, A. Aravind, Photocatalytic dye degradation efficiency of Co doped ZnO nanostructure, IOP Conf. Ser.: Mater. Sci. Eng., 1263 (2022) 012010, doi: 10.1088/1757-899X/1263/1/012010.
[9] K. Aravinthkumar, I. John Peter, G. Anandha Babu, M. Navaneethan, S. Karazhanov, C. Raja Mohan, Enhancing the short circuit current of a dye-sensitized solar cell and photocatalytic dye degradation using Cr doped $SrTiO_3$ interconnected spheres, Mater. Lett., 319 (2022) 132284, doi: 10.1016/j.matlet.2022.132284.
[10] J. Jin, H.S. Li, W.F. Yan, Y.C. Wang, Q.A. Qiao, Q.J. Zhang, S.Y. Wu, Y.H. Lu, S.F. Ping, Z.Y. Jiang, Synthesis, structure and photocatalytic property of a novel Zn(II) coordination polymer based on *in situ* synthetized pyridine-3,4-dicarboxylhydrazidate ligand, Spectrochim. Acta, Part A, 233 (2020) 118232, doi: 10.1016/j.saa.2020.118232.

[11] J. Jin, W.F. Yan, Q.F. Yang, X.T. Yu, L.X. Sun, J.Q. Xu, Z.A. Chen, C.Z. Li, New oxalate-propagated layered Mn^{2+}/Fe^{2+}-4,4-sulfoyldiphthalhydrazidate coordination polymers, J. Mol. Struct., 1127 (2017) 303–308.
[12] J. Jin, H. Chen, X. Zhang, Y.C. Wang, Z.J. Zhang, Q.F. Yang, C. Lin, J.R. Li, Q.J. Zhang, Synthesis, structural characterization and photoluminescence property of two Zn^{2+}/In^{3+}-4,4′-oxydiphthalhydrazidate complexes, Inorg. Chim. Acta, 482 (2018) 1–7.
[13] W. Hu, C. Rao, G. Ye, C. Chen, X. Wu, M. Muddassir, A. Singh, Photocatalytic organic dye by two new coordination polymers with flexible dicarboxylate and different N-donor linkage, Inorg. Chim. Acta, 519 (2021) 120284, doi: 10.1016/j.ica.2021.120284.
[14] J.J. Lu, Y. Liu, H.Y. Lin, Z.W. Cui, Q.Q. Liu, X.L. Wang, Metal and bis(pyridyl)-bis(amide) ligands – tuned three new nickel(II)/copper(II) coordination polymers: Syntheses, structures and properties, Polyhedron, 216 (2022) 115699, doi: 10.1016/j.poly.2022.115699.
[15] R. Dridi, S.N. Cherni, F. Fettar, N. Chniba-Boudjada, M.F. Zid, A novel oxalate-based three-dimensional polymorphs supramolecular compounds: synthesis, spectroscopic characterization, magnetic and photocatalytic properties, J. Mol. Struct., 1205 (2020) 127573, doi: 10.1016/j.molstruc.2019.127573.
[16] R.H. Hou, P. Han, Q. Liu, G.R. Xu, S.J. Xu, T. Chen, A new Zn(II)-coordination polymer based on m-terphenyl pentacarboxylic acid ligand for photocatalytic methylene blue degradation and protective effect against Alzheimer's disease by reducing the inflammatory response and oxidative stress in the nerve cells, Arabian J. Chem., 13 (2020) 5171–5180.
[17] M. Muslim, A. Ali, I. Neogi, N. Dege, M. Shahid, M. Ahmad, Facile synthesis, topological study, and adsorption properties of a novel Co(II)-based coordination polymer for adsorptive removal of methylene blue and methyl orange dyes, Polyhedron, 210 (2021) 115519, doi: 10.1016/j.poly.2021.115519.
[18] S.E.D.H. Etaiw, H. Marie, 3D-Supramolecular coordination polymer nanoparticles based on Cd(II) and mixed ligands: single crystal X-ray structure, luminescence and photocatalytic properties, J. Inorg. Organomet. Polym., 28 (2018) 508–518.
[19] G.L. Li, W.D. Yin, Q.L. Liu, X.R. Gong, Y.J. Zhao, G.Z. Liu, N-donor-induced two Co(II) coordination polymers derived from the flexible citraconic acid as photocatalysts for the decomposition of organic dyes, J. Inorg. Gen. Chem., 648 (2022) e202100037, doi: 10.1002/zaac.202100037.
[20] R. Feyerherm, A. Loose, M.A. Lawandy, J. Li, Structural and magnetic ordering in the two-dimensional coordination polymer Co(ox)(bpy-d8), (ox = $C_2O_4^{2-}$, bpy-d8 = 4,4′-bipyridine-d8), J. Phys. Chem. Solids, 63 (2002) 71–77.
[21] I. Mantasha, S. Hussain, M. Ahmad, M. Shahid, Two dimensional (2D) molecular frameworks for rapid and selective adsorption of hazardous aromatic dyes from aqueous phase, Sep. Purif. Technol., 238 (2020) 116413, doi: 10.1016/j.seppur.2019.116413.
[22] J. Jin, Y.C. Wang, W.F. Yan, C. Wang, W.L. Wang, Y.Z. Niu, B.Q. Yuan, H. Xu, H.S. Li, Q.J. Zhang, Synthesis and properties of Mg^{2+} and Sr^{2+} coordination compounds based on *in situ* synthetized pyromellitdihydrazidate ligand, J. Mol. Struct., 1204 (2020) 127560, doi: 10.1016/j.molstruc.2019.127560.
[23] W.H. Mahmoud, G.G. Mohamed, S.Y.A. Sabrine, Spectroscopic characterization, thermal, antimicrobial and molecular docking studies on nano-size mixed ligand complexes based on sudan III azodye and 1,10-phenanthroline, J. Therm. Anal. Calorim., 130 (2017) 2167–2184.
[24] A.C. Tella, V.T. Olayemi, F.A. Adekola, A.C. Oladipo, V.O. Adimula, J.O. Ogar, E.C. Hosten, A.S. Ogunlaja, S.P. Argent, R. Mokaya, Synthesis, characterization and density functional theory of copper(II) complex and cobalt(II) coordination polymer for detection of nitroaromatic explosives, Inorg. Chim. Acta, 515 (2021) 120048, doi: 10.1016/j.ica.2020.120048.
[25] R. Luo, C.G. Xu, G.B. Chen, C.Z. Xie, P. Chen, N. Jiang, D.M. Zhang, Y.H. Fan, F. Shao, Four novel cobalt(II) coordination polymers based on anthracene-derived dicarboxylic acid as multi-functional fluorescent sensors toward different inorganic ions, Cryst. Growth Des., 23 (2023) 2395–2405.
[26] Y.N. Wang, H. Xu, S.D. Wang, R.Y. Mao, L.J. Liu, L.M. Wen, S.Y. Wang, Y. Sun, Q.F. Yang, 1,2,4-Triazole controlled Co(II) coordination polymer with highly fluorescent sensitive detection behavior of acetylacetone, Inorg. Chim. Acta, 556 (2023) 121621, doi: 10.1016/j.ica.2023.121621.
[27] B. Nayak, S. Baruah, A. Puzari, 1D copper(II) based coordination polymer/PANI composite fabrication for enhanced photocatalytic activity, J. Photochem. Photobiol., A, 427 (2022) 113803, doi: 10.1016/j.jphotochem.2022.113803.
[28] S. Sakthivel, B. Neppolian, M.V. Shankar, B. Arabindoo, M. Palanichamy, V. Murugesan, Solar photocatalytic degradation of azo dye: comparison of photocatalytic efficiency of ZnO and TiO_2, Sol. Energy Mater. Sol. Cells, 77 (2003) 65–82.
[29] J.J. Wang, L.B. Wang, Z. Cao, E.L. Yue, L. Tang, X. Wang, X.Y. Hou, Y.Q. Zhang, Four coordination polymers based on 5-(3,5-dicarboxybenzyloxy) isophthalic acid: synthesis, structures, photocatalytic properties, fluorescence sensing and magnetic properties, J. Solid State Chem., 302 (2021) 122379, doi: 10.1016/j.jssc.2021.122379.
[30] H.N. Abid, A. Al-Keisy, D.S. Ahmed, A.T. Salih, A. Khammas, pH dependent synthesis and characterization of bismuth molybdate nanostructure for photocatalysis degradation of organic pollutants, Environ. Sci. Pollut. Res., 29 (2022) 37633–37643.
[31] M. Deng, J. Xue, P. Xie, H. Huang, J.Q. Liu, Y. Zhou, Z.H. Chen, Y.G. Ma, A new Co(II)-based coordination polymer for photocatalytic degradation of organic dyes and protective effect on spinal cord injury by increasing *trka* receptor gene expression on the NSCs, J. Inorg. Organomet. Polym., 30 (2020) 3213–3220.
[32] Y.W. Gao, S.M. Li, Y.X. Li, L.Y. Yao, H. Zhang, Accelerated photocatalytic degradation of organic pollutant over metal-organic framework MIL-53(Fe) under visible LED light mediated by persulfate, Appl. Catal., B, 202 (2017) 165–174.
[33] M. Gopannagari, D.P. Kumar, H. Park, E.H. Kim, P. Bhavani, D.A. Reddy, T.K. Kim, Influence of surface-functionalized multi-walled carbon nanotubes on CdS nanohybrids for effective photocatalytic hydrogen production, Appl. Catal., B, 236 (2018) 294–303.
[34] Y. Gao, S. Li, Y. Li, L. Yao, H. Zhang, Accelerated photocatalytic degradation of organic pollutant over metal-organic framework MIL-53 (Fe) under visible LED light mediated by persulfate, Appl. Catal., B, 202 (2017) 165–174.

Supporting information

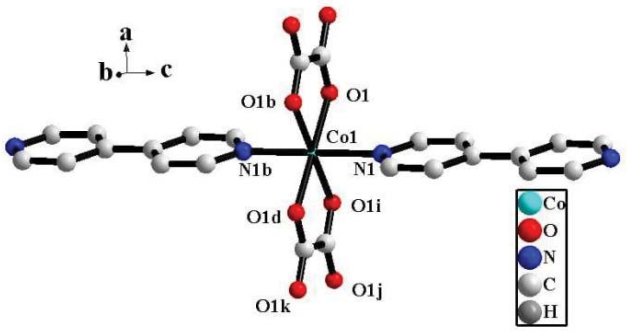

Fig. S1. Coordination environment of Co^{2+} center for compound 1 (symmetric code b: *x*, –*y* + 1, –*z*; d: –*x* + 1, –*y* + 1, *z*; i: –*x* + 1, *y*, –*z*; j: *x*–1, *y*, *z*, k: *x*–1, –*y* + 1, –*z*; l: *x*, *y*, *z*–1).

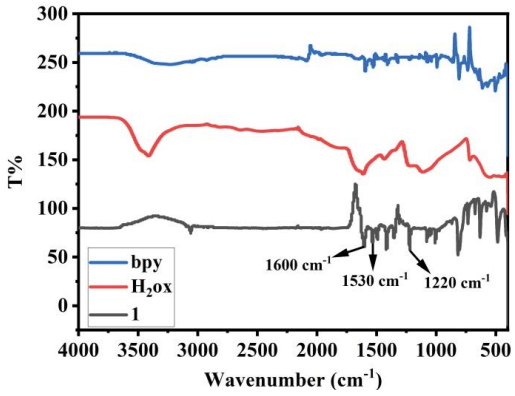

Fig. S2. Infrared spectrum of compound 1, bpy and H_2ox.

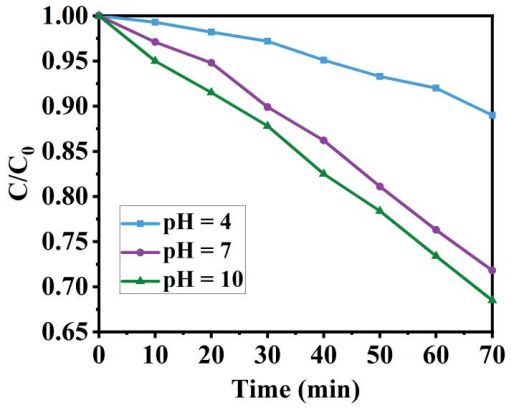

Fig. S3. Self-degradation efficiency of methylene blue (pH = 4: 11%; pH = 7: 28.2%; pH = 31.5%).

Datablock 1

Bond precision:	C–C = 0.0070 Å		Wavelength = 0.71073
Cell:	a = 5.4021(5)	b = 10.9756(11)	c = 11.3896(10)
	α = 90	β = 90	γ = 90
Temperature:	293 K		

	Calculated	Reported
Volume	675.30(11)	675.30(11)
Space group	I_{mmm}	I_{mmm}
Hall group	$-I_{22}$	$-I_{22}$
Moiety formula	$C_{12}H_8CoN_2O_4$	$C_{12}H_8CoN_2O_4$
Sum formula	$C_{12}H_8CoN_2O_4$	$C_{12}H_8CoN_2O_4$
M_r	303.13	303.13
D_x, g/cm^3	1.491	1.491
Z	2	2
Mu (mm^{-1})	1.280	1.280
$F000$	306.0	306.0
$F000'$	306.83	
h,k,l_{max}	6,13,13	6,13,13
N_{ref}	372	366
T_{min}, T_{max}	0.858,0.880	
T_{min}'	0.858	

Correction method = Not given

Data completeness = 0.984 θ(max) = 25.098

R(reflections) = 0.0355(353) $wR2$(reflections) = 0.1241(366)

S = 1.452 N_{par} = 41

The following ALERTS were generated. Each ALERT has the format
test-name_ALERT_alert-type_alert-level.
Click on the hyperlinks for more details of the test.

Alert level C

PLAT052_ALERT_1_C Info on Absorption Correction Method Not Given Please Do!
PLAT088_ALERT_3_C Poor Data/Parameter Ratio …… 9.07 Note
PLAT250_ALERT_2_C Large U3/U1 Ratio for Average $U(i,j)$ Tensor …… 2.1 Note
PLAT341_ALERT_3_C Low Bond Precision on C–C Bonds …… 0.007 Ang

Alert level G

PLAT004_ALERT_5_G Polymeric Structure Found with Maximum Dimension …… 2 Info
PLAT012_ALERT_1_G No _shelx_res_checksum Found in CIF …… Please Check
PLAT199_ALERT_1_G Reported _cell_measurement_temperature …… (K) 293 Check
PLAT200_ALERT_1_G Reported _diffrn_ambient_temperature …… (K) 293 Check
PLAT300_ALERT_4_G Atom Site Occupancy of C2 Constrained at 0.5 Check
And 3 other PLAT300 Alerts
More ...
PLAT301_ALERT_3_G Main Residue Disorder …… (Resd 1) 34% Note
PLAT789_ALERT_4_G Atoms with Negative _atom_site_disorder_group # 4 Check
PLAT822_ALERT_4_G CIF-embedded. res Contains Negative PART Numbers 1 Check
PLAT883_ALERT_1_G No Info/Value for _atom_sites_solution_primary. Please Do!
PLAT967_ALERT_5_G Note: 2θ Cutoff Value in Embedded. res …… 50.2°